Determining the photoelectric parameters of an organic photoconductor by the photoelectromotive-force technique

M. C. Gather,[1] S. Mansurova,[1,2] and K. Meerholz[1]
[1]*Insitut für Physikalische Chemie, Luxemburger Strasse 116, Köln 50939, Germany*
[2]*INAOE, Apartado Postal 51 y 216, Puebla 72000, México*
(Received 24 July 2006; revised manuscript received 20 December 2006; published 9 April 2007)

We report on a theoretical model to describe the non-steady-state photoelectromotive-force (photo-EMF) effect in organic photoconductors. Unlike the conventional theory of the photo-EMF effect developed for crystalline materials, this model accounts for the field dependence of the charge generation quantum efficiency and charge carrier mobility. To verify our findings a detailed experimental study of the charge carrier generation and transport processes in a organic photorefractive composite was performed using the photo-EMF effect and ac photocurrent measurements. The investigated composite was based on a conjugated triphenyldiamine based polymer (TPD-PPV) sensitized with a highly soluble fullerene derivative (PCBM). Our results show that at zero and low dc field the dependence of the photo-EMF signal on frequency, grating period and external electric field is well described by the standard model originally developed for an inorganic monopolar photoconductor with finite charge carrier lifetime. In this regime the photo-EMF effect was used to determine zero- and low-field photoelectric material parameters including the low-field hole mobility ($\mu_{0,h}=1.3\times10^{-4}$ cm^2/V s), the effective charge carrier lifetime ($\tau=45$ μs), the diffusion length ($L_D=114$ nm), and the primary charge carrier generation efficiency ($\Phi=5.3\times10^{-3}\%$). In addition, the validity of the Einstein relation ($D/\mu=25$ meV) was verified for the low-field regime. At high electric fields the signal behavior deviates significantly from the trend predicted by the standard model for inorganic photoconductors. This behavior which is mainly attributed to the strong field dependence of the charge generation rate is well described by our model.

DOI: 10.1103/PhysRevB.75.165203 PACS number(s): 72.80.Le, 72.20.Jv, 42.70.Jk, 72.40.+w

I. INTRODUCTION

Today organic semiconductors are considered as active components for a wide range of electro-optic devices, including solar cells,[1] field effect transistors,[2] light emitting diodes,[3] holographic storage media,[4] and laser diodes.[5] Among the main reasons for the strong interest in this class of materials are their compatibility with low cost fabrication processes, the inherent mechanical flexibility and the tunability of their properties by chemical modification or blending.

Understanding and characterizing the photophysical properties of organic materials is one of the main challenges in this field of research. Here, we demonstrate an alternative characterization technique which is based on the periodic excitation of the excess charge carriers created by two interfering laser beams. The most important feature of this technique is the interaction between the photoinduced space charge field grating and the grating of mobile photocarriers which results in a periodic current flowing through the sample. Numerous characterization techniques based on this principle emerged during the last two decades (e.g., steady-state photocarrier grating,[6] transient grating,[7] moving photocarrier grating[8]). They have been successfully used for the investigation of the photoconductive properties of inorganic crystalline and amorphous materials.

One of the most successful techniques in this group is based on the so-called non-steady-state photoelectromotive force (photo-EMF) effect.[9] Here, one measures the ac current resulting from the illumination of the sample with an oscillating interference pattern. The technique was applied to a variety of crystalline inorganic materials (such as GaAs,[10] $LiNbO_3$,[11] $B_{12}TiO_{20}$,[12] and multiple quantum well structures[13]) and proved to be a powerful tool for the determination of important photoelectrical parameters such as the photocarrier drift and diffusion length (L_0, L_D), the mobility (μ) and the charge carrier lifetime (τ). In addition, this technique is suitable for material characterization in a wide range of electric fields (starting from zero field) and allows for an easy modification of the spatial and the temporal scale of the measurement by changing the period of the interference fringes or the frequency of oscillation.

Recently, we have demonstrated that the photo-EMF technique can also be used for characterization of amorphous organic materials.[14,15] However, our results indicated that the theoretical model of the photo-EMF effect originally developed for inorganic crystalline materials requires significant modification before it can adequately describe the situation in organic materials.

The main reason for this is that many of the relevant processes in organic, often highly disordered semiconductors differ fundamentally from their inorganic, mostly crystalline counterparts. The charge transport, for example, is mediated by hopping processes due to the strong charge confinement being present in organic semiconductors.[16] This localization of states also results in a relatively large exciton binding energy which causes a strong field dependence of the charge generation efficiency. Theoretical modelling and systematic experimental investigation of the space charge grating formation in organic amorphous photoconductors are, therefore, essential for the future use of the photo-EMF technique in this field.

In the first part of this paper we introduce a theoretical model to describe the photo-EMF effect in organic photocon-

ductors, taking into account the field dependence of the charge carrier generation and mobility in these materials. The second part compares the predictions made by this model with experimental data. The investigations were performed on a fullerene sensitized photoconductive composite based on the hole-conducting conjugated copolymer of triphenyldiamine and phenylenevinylene (TPD-PPV).[17,18] The electroluminescent green-emitting TPD-PPV was chosen as a model system due to its relatively high mobility, which renders the material an interesting candidate for electrically pumped lasers, photovoltaic devices, and organic field effect transistors. Mixtures of TPD-PPV with electro-optic chromophores and a small amount of PCBM (1 wt %) were reported as a very efficient holographic recording medium.[19]

II. THEORETICAL ANALYSIS

In this section we derive the main theoretical expressions for the non-steady-state photo-EMF current density in organic photoconductors. The energy structure we assume is similar to the structure assumed in the Schildkraut model: Optically generated electron-hole pairs are separated by electron accepting sensitizer molecules (with a concentration N^S) leaving mobile positive charges (with an effective concentration p) on the neighboring hole transport molecules.[20] Drift and diffusion forces lead to subsequent charge transport before the excited holes recombine with negatively charged sensitizer molecules (with a concentration of N_S^-). In contrast to the conventional theory we assume that charge generation efficiency Φ and charge carrier mobility μ have an arbitrary field dependence, i.e., $\Phi=\Phi(E)$ and $\mu=\mu(E)$. The following set of equations can be used to describe the activation, recombination, and transport process of holes under a constant electric dc field E_0:

$$\frac{\partial p}{\partial t} = s\Phi I(N_S - N_S^-) - \gamma p N_S^- - \frac{\partial (j/e)}{\partial x}, \tag{1}$$

$$\frac{\partial N_S^-}{\partial t} = s\Phi I(N_S - N_S^-) - \gamma p N_S^-, \tag{2}$$

$$j = e\mu p E - eD\frac{\partial p}{\partial x}, \tag{3}$$

$$\frac{\partial E}{\partial x} = \frac{e}{\varepsilon\varepsilon_0}(p - N_S^-). \tag{4}$$

Here e is the elementary charge, s is the optical absorption cross section, I is the incident light intensity, γ is the coefficient of hole recombination, j is the current density, D is the charge carrier diffusion coefficient, $E=E_0+E_{sc}$ is the local value of the total electric field and $\varepsilon\varepsilon_0$ is the dielectric constant of the material. E_{sc} is the space charge field. If saturation of the activation-recombination centers is neglected Eqs. (1) and (2) can be reduced to the following form:

$$\frac{\partial p}{\partial t} = g - \frac{p}{\tau} - \frac{\partial (j/e)}{\partial x}, \tag{5}$$

$$\frac{\partial N_s^-}{\partial t} = g - \frac{p}{\tau}. \tag{6}$$

Here $g=s\Phi I(N_S-N_S^-)$ is the charge generation rate and $\tau=1/(\gamma N_S^-)$ is the effective average lifetime of mobile holes under uniform illumination.

Combining Eqs. (1)–(6) we arrive at a system of two nonlinear differential equations for the concentration of mobile holes $p(x,t)$ and the electric field distribution $E(x,t)$,

$$\frac{\partial^2 E}{\partial x \partial t} = -\frac{e}{\varepsilon\varepsilon_0}\left(\mu p\frac{\partial E}{\partial x} + \mu E\frac{\partial p}{\partial x} + Ep\frac{\partial \mu}{\partial x} - D\frac{\partial^2 p}{\partial x^2}\right), \tag{7}$$

$$\frac{\partial p}{\partial t} = g - \frac{p}{\tau} - \left(\mu p\frac{\partial E}{\partial x} + \mu E\frac{\partial p}{\partial x} + Ep\frac{\partial \mu}{\partial x} - D\frac{\partial^2 p}{\partial x^2}\right). \tag{8}$$

Note, that neither the hole mobility (μ), nor the quantum yield of charge carrier generation (Φ) depend explicitly on the spatial coordinate x, but that there is only an indirect dependence which results from the dependence of μ and Φ on the electric field,

$$\frac{\partial \mu}{\partial x} = \frac{\partial \mu}{\partial E}\frac{\partial E}{\partial x}, \tag{9}$$

$$\frac{\partial \Phi}{\partial x} = \frac{\partial \Phi}{\partial E}\frac{\partial E}{\partial x}. \tag{10}$$

Now we consider the illumination of the material by an oscillating interference pattern which is formed by two coherent plane waves one of which is periodically modulated in phase with a frequency Ω and an amplitude Δ. The spatial distribution of the incident intensity is then given by

$$I(x) = I_0\{1 + m\cos[Kx + \Delta\cos(\Omega t)]\}. \tag{11}$$

Here I_0 is the average light intensity, K is the spatial frequency of the pattern, and m is the effective contrast of the interference fringes. In the regime of small amplitude of phase modulation ($\Delta \ll 1$) the complex representation of the intensity distribution can be used

$$\begin{aligned} I(x) = {} & I_0 + I^{10}\exp(iKx) + I^{11}\exp[i(Kx+\Omega t)] \\ & + I^{1-1}\exp[i(Kx-\Omega t)] + I^{-10}\exp(-iKx) + I^{-1-1} \\ & \times\exp[-i(Kx+\Omega t)] + I^{-11}\exp[i(-Kx+\Omega t)], \end{aligned} \tag{12}$$

where

$$I^{10} = I^{-10} = \frac{m}{2}I_0,$$

$$I^{11} = I^{1-1} = I^{-11} = I^{-1-1} = \frac{im\Delta}{4}I_0. \tag{13}$$

Here the upper indices denote the spatial and temporal harmonic of the corresponding complex amplitude; a negative sign in the upper index indicates complex conjugation of the respective harmonic. For example, I^{11} is the complex amplitude of the first spatial and first temporal harmonic.

We can now develop solutions for $E(x,t)$ and $p(x,t)$ which are in form identical to the intensity decomposition

given in Eq. (12). Assuming small fringe contrast ($m<1$) and ignoring all terms proportional to m^2 we can linearize Eqs. (7) and (8). A detailed justification for this assumption is given, for example, by Stepanov.[21] For the linearization procedure the following linear approximations of the field dependent mobility and charge generation efficiency are used,

$$\mu(E) \approx \mu(E_0) + \left.\frac{\partial \mu}{\partial E}\right|_{E_0} E_{sc}, \tag{14}$$

$$\Phi(E) \approx \Phi(E_0) + \left.\frac{\partial \Phi}{\partial E}\right|_{E_0} E_{sc}. \tag{15}$$

The complex amplitudes for the concentration of holes p and the space charge field E_{sc} can now be expressed as

$$E_{sc}^{10} = \frac{m}{\eta(E_0)}(iE_D - E_0), \tag{16}$$

$$p^{10} = mp_0, \tag{17}$$

$$E_{sc}^{11} = \frac{i\Delta m}{4}\frac{(iE_D - E_0)/\eta(E_0)}{1 + i\Omega[\tau + \tau_{di}(1 + K^2L^2{}_D + iKL_0)/\eta(E_0)] - \Omega^2\tau\tau_{di}/\eta(E_0)}, \tag{18}$$

$$p^{11} = \frac{i\Delta m}{4}p_0\frac{[1 + i\Omega\tau_{di}/\eta(E_0)]}{1 + i\Omega[\tau + \tau_{di}(1 + K^2L^2{}_D + iKL_0)/\eta(E_0)] - \Omega^2\tau\tau_{di}/\eta(E_0)}. \tag{19}$$

Here $E_D = KD/\mu$, L_D is the diffusion length and L_0 is the drift length of the charge carriers. $\tau_{di} = \varepsilon\varepsilon_0/\sigma$ is the dielectric relaxation time reflecting how fast the carriers relax to equilibrium distribution. $\sigma = s\Phi I\mu\tau e$ is the average photoconductivity.

Equations (16)–(19) are similar to the expressions derived for inorganic crystals[21] with the important extension of the dimensionless coefficient $\eta(E_0)$,

$$\eta(E_0) = 1 + \frac{E_0}{\Phi(E_0)}\left.\frac{\partial \Phi}{\partial E}\right|_{E_0} + \frac{E_0}{\mu(E_0)}\left.\frac{\partial \mu}{\partial E}\right|_{E_0} - i\frac{E_D}{\Phi(E_0)}\left.\frac{\partial \Phi}{\partial E}\right|_{E_0} \tag{20}$$

which accounts for the contribution of the field dependence of mobility and charge carrier generation efficiency.

The fundamental harmonic of the photo-EMF current density can then be calculated using the following combination of amplitudes:

$$j^{\Omega}_{p\text{-emf}} = \frac{e\mu}{2}(E_{sc}^{11}p^{-10} + E_{sc}^{-10}p^{11} + E_{sc}^{-11}p^{10} + E_{sc}^{10}p^{-11}). \tag{21}$$

Substituting Eqs. (16)–(20) into Eq. (21) the final expression for the photo-EMF current density can be written as

$$j^{\Omega}_{p\text{-emf}} = \frac{\Delta m^2}{4}\frac{\sigma_0(E_0)}{|\eta(E_0)|^2}\left(\frac{2i\{E_D\,\mathrm{Im}[\eta(E_0)] + E_0\,\mathrm{Re}[\eta(E_0)]\} + \Omega\tau_{di}(iE_D + E_0)}{1 + i\Omega[\tau + \tau_{di}(1 + K^2L^2{}_D + iKL_0)/\eta(E_0)] - \Omega^2\tau\tau_{di}/\eta(E_0)} + \frac{2i\{E_D\,\mathrm{Im}[\eta(E_0)] + E_0\,\mathrm{Re}[\eta(E_0)]\} - \Omega\tau_{di}(iE_D - E_0)}{1 + i\Omega[\tau + \tau_{di}(1 + K^2L^2{}_D - iKL_0)/\eta^*(E_0)] - \Omega^2\tau\tau_{di}/\eta^*(E_0)}\right). \tag{22}$$

It is important to note that all above expressions were derived in the rather general approximation of small contrast of the interference fringes ($m<1$) and small amplitude of phase modulation ($\Delta<1$). No specific assumptions were made about the energetic depth and occupation of the electron trapping centers or about the form of the field dependence of the photoconductivity parameters. This allows the potential use of Eqs. (16)–(19) and (22) for a variety of materials as long as the quasineutrality condition remains valid.

In the following, we will analyze the results obtained above for two different dc field regimes: (1) at zero dc field and in the low-field regime, i.e., when Φ and μ are not field dependent, and (2) at high dc fields when $\Phi = \Phi(E_0)$ and $\mu = \mu(E_0)$.

A. Zero ($E_0=0$) and low dc field (Φ, $\mu\approx$const)

If the Φ and μ are not field dependent the field factor $\eta(E_0)$ becomes unity and Eq. (22) reduces to the well-known form of the photo-EMF current density,

$$j^{\Omega}_{p\text{-emf}} = \frac{\Delta m^2}{4}\sigma_0\left(\frac{2iE_0+\Omega\tau_{di}(iE_D+E_0)}{1+i\Omega[\tau+\tau_{di}(1+K^2L^2{}_D+iKL_0)]-\Omega^2\tau\tau_{di}} - \frac{2iE_0-\Omega\tau_{di}(iE_D-E_0)}{1+i\Omega[\tau+\tau_{di}(1+K^2L^2{}_D-iKL_0)]-\Omega^2\tau\tau_{di}}\right) \quad (23)$$

for inorganic monopolar photoconductors with finite photocarrier lifetime.[21] This indicates that at least for low dc fields the theoretical tools developed for inorganic crystalline materials are also valid for amorphous organic materials and that they can be used to characterize the material at low dc fields. Note, that the direct determination of photoelectric parameters at low dc fields is not possible by any of the techniques which are commonly used for the characterization of organic semiconductors (e.g., TOF, corona discharge, etc.).

In the following, we describe the experimental dependencies of $j^{\Omega}_{p\text{-emf}}$ for the case of a relaxation type photoconductor ($\tau_{di}\gg\tau_h$) since this is the relevant case for the analysis of the experimental results discussed later.

For intermediate frequencies of modulation ($\tau_{di}{}^{-1}\ll\Omega\ll\tau^{-1}$) the field dependence of the signal can be expressed as

$$j^{\Omega}_{p\text{-emf}}(E_0) = \frac{m^2\Delta}{2}\sigma_0 E_D\frac{E_D(1+K^2L_D^2)-KL_0E_0}{(1+K^2L_D^2)^2+K^2L_0^2}. \quad (24)$$

It can be seen that $j^{\Omega}_{p\text{-emf}}$ changes sign if the numerator of Eq. (24) vanishes. Note, that since the absolute value of $j^{\Omega}_{p\text{-emf}}$ is the quantity that is experimentally accessible we expect a minimum of the signal at this point. Assuming small spatial frequencies ($KL_D\ll 1$) the term KL_D can be neglected and the change of sign is expected at an external field $E_0'=(1/\mu\tau)\times(D/\mu)^{1/2}$. It can be easily seen that at this point drift and diffusion length are equal ($L_D=L_0$). If the Einstein relation between the diffusion coefficient and the mobility is fulfilled (i.e., $D/\mu=k_bT/e=25$ meV) the $\mu\tau$ product and the diffusion length are directly related to E_0',

$$\mu\tau = \frac{1}{E_0'^2}\frac{k_BT}{e},$$

$$L_D = \frac{1}{E_0'}\frac{k_BT}{e}. \quad (25)$$

As τ can be readily determined from frequency domain photocurrent measurements this relation provides a very interesting tool for the determination of the charge carrier mobility and the diffusion coefficient. However, it is well known that the Einstein relation is not generally fulfilled in organic semiconductors due to their often dispersive charge transport characteristics.[15,22–24] In order to determine the D/μ ratio of a material it has been proposed to measure the absolute value of the photocurrent $j^{\Omega}_{ph}=\sigma_0E_{0,ph}$ under experimental conditions identical to the photo-EMF experiment (i.e., at the same wavelength, average intensity, and geometry, and at low external field E_0).[15] Normalizing Eq. (23) with j^{Ω}_{ph} gives an expression which does not depend on the photoconductivity σ_0 anymore,

$$\frac{J^{\Omega}_{p\text{-emf}}}{J^{\Omega}_{ph}} = \frac{j^{\Omega}_{p\text{-emf}}}{j^{\Omega}_{ph}} = \frac{m^2\Delta}{2E_{0,ph}}K\frac{D}{\mu}. \quad (26)$$

However, the method still requires measuring the absolute value of the signal. This may lead to experimental errors difficult to account for, e.g., internal reflection from electrodes, nonperfect beam overlap, changes of the effective contrast due to absorption.

Therefore, in this work a simpler method which does not require the knowledge of the absolute value of the photo-EMF signal is proposed. Let us consider the field dependence of $j^{\Omega}_{p\text{-emf}}$ [cf. Eq. (24)] for the case of small spatial periods $KL_D\gg 1$. The minimum of the signal occurs at an external field E_0'' which equals the diffusion field ($E_0''=E_D=KD/\mu$). Consequently, the D/μ ratio is simply given by E_0''/K. This relation provides a very direct and robust test of the Einstein relation as it only requires the knowledge of the applied field and of the angle of the incident beams. The intrinsic limitation of this method is that it can be used only in materials with relatively long diffusion lengths ($L_D\geqslant\lambda/4\pi$), where the condition of small spatial periods ($KL_D\ll 1$) is accessible for reasonable beam crossing angles.

B. High dc field [$\Phi=\Phi(E_0), \mu=\mu(E_0)$]

Since the analysis of Eq. (22) at high dc field is rather complicated, we will again restrict the discussion to the case of relaxation type photoconductors where the dielectric relaxation time is much longer than the effective charge carrier lifetime ($\tau_{di}\gg\tau$) and to the optimal frequency regime, i.e., where the observed photo-EMF signal is maximal ($\tau_{di}{}^{-1}\ll\Omega\ll\tau^{-1}$). In this limit the expression for the photo-EMF current density amplitude reduces to

$$j^{\Omega}_{p\text{-emf}} = \frac{\Delta m^2}{2}\frac{\sigma(E_0)}{|\eta(E_0)|^2}\times\frac{E_D\{(1+K^2L_D^2)\mathrm{Re}[\eta(E_0)]+KL_0\,\mathrm{Im}[\eta(E_0)]\}-E_0\{KL_0\,\mathrm{Re}[\eta(E_0)]+(1+K^2L_D^2)\mathrm{Im}[\eta(E_0)]\}}{(1+K^2L_D^2)^2+(KL_0)^2}. \quad (27)$$

Further analysis of Eq. (26) requires the knowledge of the functional dependencies of $\Phi(E_0)$ and $\mu(E_0)$ which are determined by material properties and experimental conditions. In the following we assume a power-law field dependence of the charge generation efficiency

$$\Phi(E_0) = \Phi_0(1 + aE_0^{\alpha}) \tag{28}$$

which is typical for sensitized organic photoconductors. Here Φ_0 is the primary quantum yield; α and a are phenomenological constants. A Poole-Frenkel field dependence is assumed for the mobility

$$\mu(E_0) = \mu_0 \exp(\beta E_0^{1/2}), \tag{29}$$

where μ_0 is the mobility at zero dc field and β is a phenomenological constant. Based on Eqs. (28) and (29) the factor $\eta(E_0)$ can be rewritten as

$$\eta(E_0) = 1 + \alpha\frac{aE^{\alpha}}{1 + aE^{\alpha}} + \frac{\beta E_0^{1/2}}{2} - i\frac{E_D}{E_0}\alpha\frac{aE_0^{\alpha}}{1 + aE_0^{\alpha}}. \tag{30}$$

The imaginary part of $\eta(E_0)$ goes to zero with increasing dc field and can hence be neglected. The real part, however, grows as the square root of the applied dc field and must be taken into account. If we also assume the case of large drift lengths ($KL_0 > 1$) the above expression simplifies even more,

$$j_{p\text{-emf}}^{\Omega} \cong \frac{\Delta m^2}{2}\frac{e\Phi(E_0)}{K\,\mathrm{Re}\;\eta(E_0)}. \tag{31}$$

This shows that, as a result of the field dependence of the photoconductivity parameters in organics (especially the charge generation efficiency), the behavior of the photo-EMF current under large dc bias can deviate significantly from the situation typical for inorganic materials. Note that for inorganic materials the photo-EMF signal is constant in the limiting case of large drift length:

$$j_{p\text{-emf}}^{\Omega} \cong (\Delta m^2/2)e\Phi/K. \tag{32}$$

Another interesting effect arising from the field dependence of the photoconductivity parameters is that the dynamics of the recording process will also change. In particular it is interesting to investigate the resonances of the frequency transfer function of the photo-EMF signal, which are associated with "running waves" appearing as eigenmodes of the photoconductive medium in the transient regime.[25] However, the phenomenon is beyond the scope of this paper and will be reported elsewhere.

III. EXPERIMENTAL DETAILS

The material under investigation consists of the polymer poly(triphenyldiamine-co-phenylenevinylene) (TPD-PPV) (56 wt. %, see Fig. 1 for the chemical structure), an eutectic mixture of the two azo-dyes 2,5-dimethyl-4-(4′-nitrophenylazo)-anisole (DMNPAA) and 3-methoxy-4-(4′-nitrophenylazo)-anisole (MNPAA) (15 wt. % each) and the highly soluble C_{60} derivative PCBM (1 wt. %). Due to their low oxidation potential the azo-dyes are not expected to participate directly in the charge generation and transport process. Although their presence is not required for our study the chromophores were added to the composite to ensure comparability with earlier studies.[4,19]

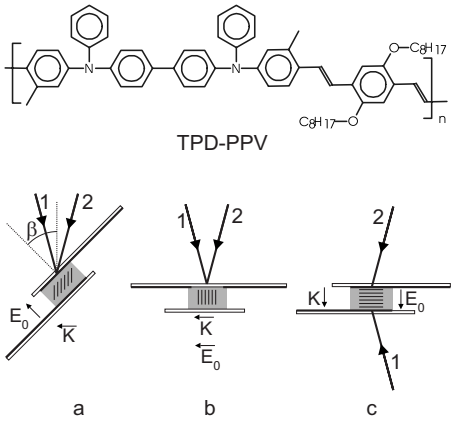

FIG. 1. Top: Molecular structure of the TPD-PPV polymer used in this work. Bottom: Schematic illustration of the three different experimental setups used for the photo-EMF measurements: (a) Conventional transmission configuration; the tilt between sample normal and bisector of the incident beams is required to obtain a component of the grating vector **K** in the direction of the collecting electrodes. (b) Transversal configuration; the need for a sample tilt is avoided as the grating vector is parallel to the collecting electrodes. (c) In reflection configuration large spatial frequencies can be achieved.

Samples with a thickness of 54 μm were prepared by sandwiching the material between indium tin oxide (ITO) electrodes. In general a photo-EMF signal can only be observed if the grating vector has a nonzero component in the direction normal to the electrodes. As both beams were incident on the sample from the same side (transmission geometry) this condition can only be met if the sample is tilted against the bisector of the two incident beams [see Fig. 1(a)]. Additionally, samples with transversal electrode geometry were made to study the photo-EMF signal under symmetrical conditions and without the need to tilt the sample [see Fig. 1(b)].

The 633 nm output of a cw HeNe laser was used to illuminate the samples with an interference pattern of high fringe contrast ($m \approx 1$). The phase of one of the beams was periodically modulated by an electro-optic modulator (Conoptics 350-105). The total incident intensity was 0.8 W/cm^2 at maximum and was adjusted with a neutral density filter wheel. To allow scanning of the grating period in the conventional transmission geometry a $4f$ setup with two large aperture lenses ($A = 50$ mm, $f = 125$ mm) and a rotating mirror was used.[26] With this arrangement we were able to vary the spatial period of the interference pattern between 2 μm and 300 μm. Since measurements in the $KL_D \gg 1$ regime required grating periods below $\Lambda_0 = 800$ nm a reflection geometry setup was also employed [see Fig. 1(c)]. Conventional frequency domain photoconductivity measurements were performed by blocking one of the two beams and by modulating the other beam with a chopper wheel. To circumvent bandwidth restrictions the signal was preamplified with a low noise current preamplifier (Stanford Research SR-570)

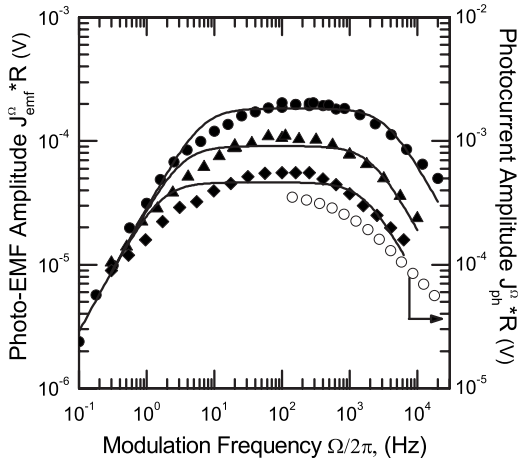

FIG. 2. The amplitude of $j^{\Omega}_{p\text{-emf}}$ as a function of the oscillation frequency of the interference grating for different light intensities: 0.8 W/cm^2 (●), 0.4 W/cm^2 (▲), 0.2 W/cm^2 (♦). The solid lines represent weighted linear regression fits to the data. The amplitude of the alternating photocurrent signal at an external field of E_0 =37 kV/cm is also shown (○).

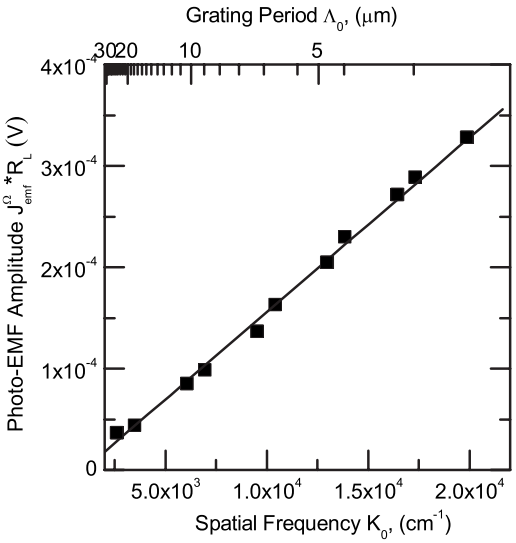

FIG. 3. The amplitude of the photo-EMF signal as a function of the spatial frequency. Modulation frequency $\Omega/2\pi$=85 Hz, modulation amplitude Δ=0.43 rad, incident intensity I=0.8 W/cm^2. The linear increase of the signal indicates that the spatial frequency of the grating is small compared to the diffusion length of the charge carriers ($KL_D \ll 1$).

before detection with a digital lock-in amplifier (Stanford Research SR-830).

IV. RESULTS AND DISCUSSION

A. Zero dc field (E_0=0)

In the following, we discuss the situation when no external electric field is applied to the sample. The theory predicts that $j^{\Omega}_{p\text{-emf}}$ maintains a constant value for modulation frequencies Ω in the range between τ_{di}^{-1} and τ^{-1} [cf. Eq. (23), assuming E_0=0, $KL_D \ll 1$]. Figure 2 shows the measured frequency dependence of the photo-EMF signal. As expected the signal falls off towards high and low frequencies and remains on a plateau for intermediate frequencies. A two parameter weighted linear regression algorithm was used to fit the data to the predicted frequency dependence and to extract the characteristic times τ_{di} and τ. To verify that τ_{di} corresponds to the dielectric relaxation time of the sample the frequency response of the photo-EMF signal was measured at different intensities (also see Fig. 2). We found τ_{di} to be inversely proportional to the intensity which is the dependence that is expected for the dielectric relaxation time. We also note, that in the intermediate frequency regime ($\tau_{di}^{-1} \ll \Omega \ll \tau^{-1}$) the amplitude of the signal depends linearly on intensity which indicates that there is no saturation of the charge carrier generation rate. For low frequencies ($\Omega\tau_{di} \ll 1$), however, the amplitude of the photo-EMF signal is intensity independent. This observation is explained by the indirect intensity dependence of Eq. (23). If the expressions for σ_0 and τ_{di} are inserted into Eq. (23) and all terms in $\Omega\tau_{di}$ and $\Omega\tau$ are neglected (which corresponds to the case of $\Omega\tau_{di} \ll 1$) the photo-EMF signal becomes intensity independent. To confirm that the second characteristic time corresponds to the effective charge carrier lifetime the frequency response at high frequencies was compared with conventional frequency domain photocurrent measurements (see open symbols in Fig. 2). We found a very good agreement between the photocurrent and the photo-EMF measurements. Note, however, that a weak negative intensity dependence of the respective characteristic time was found in both measurements. We believe that this is due to the recombination rate being influenced by the number of ionized sensitizer molecules in the material.

For an average illumination intensity of 0.8 W/cm^2 a dielectric relaxation time of τ_{di}=25±5 ms and an effective charge carrier lifetime of τ=45±6 μs ($\ll \tau_{di}$) were extracted which clearly shows that the material belongs to the class of relaxation photoconductors.

For the frequency range $\tau_{di}^{-1} \ll \Omega \ll \tau^{-1}$ we also investigated the spatial frequency dependence of the photo-EMF signal. The signal is expected to increase linearly with K if the spatial frequency is small (i.e., $KL_D \ll 1$) and to reach a maximum for $K=L_D^{-1}$. For the spatial frequency range under investigation ($K=2\times10^3-2\times10^4$ cm^{-1}) we found a strictly linear increase of $j^{\Omega}_{p\text{-emf}}$ with K (see Fig. 3 and conclude that we are working in the regime of small spatial frequencies ($KL_D \ll 1$).

B. Low dc field

As an estimate of up to which field value the low-field approximations developed in the preceding section are valid we measured the ac photocurrent signal j^{Ω}_{ph} versus external dc field E_0. Figure 4 shows the field dependence of the signal normalized to the applied field. Up to 10 kV/cm the value of j^{Ω}_{ph}/E_0 remains nearly constant, indicating that the photoconductivity is independent of E_0 below this value. Under these conditions the field dependence of the photo-EMF signal can be used to extract the diffusion length and the mobility-lifetime product using Eqs. (25). Figure 5(a) shows the

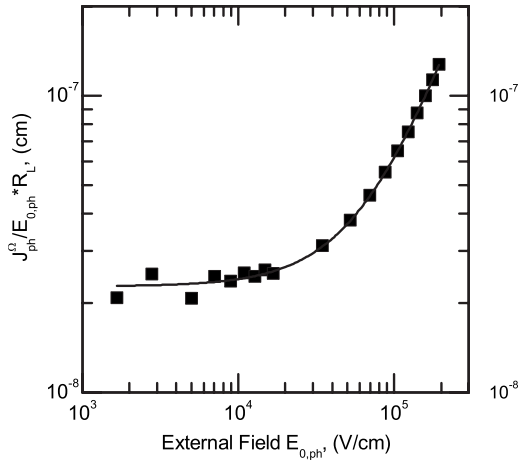

FIG. 4. Alternating photocurrent j^{Ω}_{ph} signal normalized to the applied field versus applied field $E_{0,ph}$. The chopping frequency was $\Omega/2\pi=85$ Hz, the incident intensity $I=0.4$ W/cm^2. The line represents a power-law fit reflecting the expected proportionality of $j^{\Omega}_{ph}/E_{0,ph}$ to the charge generation efficiency $\Phi(E_0)=\Phi_0(1+aE_0^{\alpha})$.

photo-EMF signal as a function of the applied electric field. As expected the amplitude of the signal decreases with field and reaches a minimum at an external field $E_0'\approx 2$ kV/cm. The phase of the photo-EMF signal is also shown in Fig. 5(a). The inflection point of the phase corresponds to the change of sign of the photo-EMF current and, therefore, provides an alternative (and more precise) method to determine E_0'. Using the phase signal we obtain $E_0'=2.2\pm0.1$ kV/cm.

As mentioned earlier the validity of the Einstein relation needs to be checked before Eqs. (25) may be used. In order to determine the D/μ ratio the field dependence of the photo-EMF signal is measured at large KL_D values which was realized in the reflection setup [see Fig. 1(c)]. The field dependence of amplitude and phase of $j^{\Omega}_{p\text{-emf}}$ is shown in Fig. 5(b). The inflection point of the phase and the minimum of the amplitude are found at an external field $E_0''=6.8\pm0.2$ kV/cm. From this measurement we obtain $D/\mu=E_0''/K=24.3$ meV for $K=4\pi n/\lambda=2.8\times10^5$ cm^{-1}) which is in excellent agreement with the theoretical expectation of $D/\mu=k_BT/e=25.2$ meV at room temperature ($T=293$ K).

Further evidence for the validity of the Einstein relation came from a comparison of the amplitude of the photo-EMF signal with the amplitude of the conventional photocurrent signal. We used samples with transversal electrodes and a normal angle of incidence [see Fig. 1(b)] to ensure a constant fringe contrast throughout the active layer of the sample. Another positive effect of this geometry is that the spatial frequency of the interference pattern is independent of the refractive index of the material. The amplitude of oscillation was set to $\Delta=0.43$ rad, which is small enough to justify the linear approximation ($j^{\Omega}_{p\text{-emf}}\propto\Delta$) used in Eq. (24). The photocurrent was measured at a moderate external field of 1.6 kV/cm, the space- and time-averaged intensity of illumination was identical for the photo-EMF and the photocurrent measurement. Using Eq. (26) a D/μ ratio of 25.7 meV was found which is again in good agreement with the theoretical expectation.[31]

In general, the validity of the Einstein relation indicates Gaussian or nondispersive charge transport. Although typical

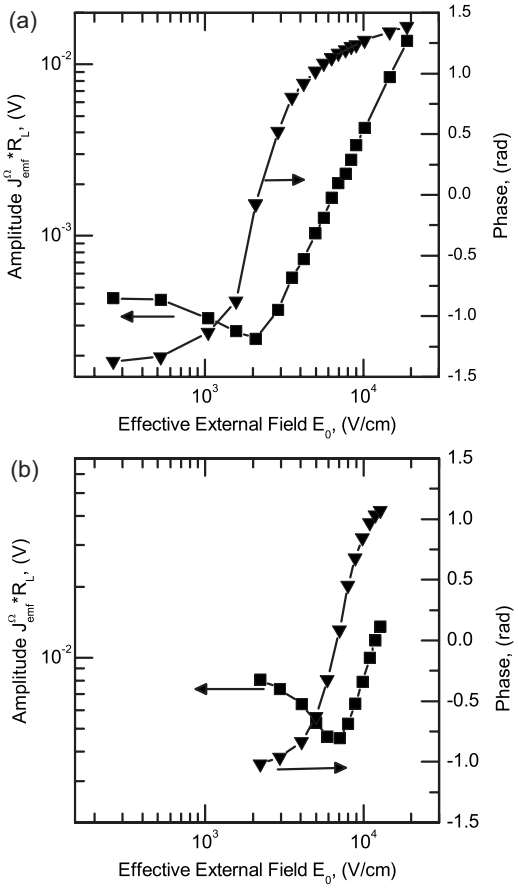

FIG. 5. (a) Field dependence of $j^{\Omega}_{p\text{-emf}}$ in the small spatial frequency regime ($KL_D\ll1$, transmission configuration). At an effective external field of $E_0'=2.2$ kV/cm the amplitude of the signal reaches a minimum and the phase passes an inflection point. (b) At large spatial frequencies ($KL_D\gg1$, reflectance configuration) minimum and inflection point are reached at an external field $E_0''=6.8$ kV/cm.

for most crystalline inorganic semiconductors this is not common for amorphous materials. However, for several materials such as poly(9,9-dioctylfluorene) and ladder-type poly-(paraphenylene), nondispersive hole transport has been observed in a certain field and temperature range.[27,28] TPD-PPV apparently falls in this class of materials, whereas this is obviously not the case for the poly(N-vinylcarbazole) (PVK) based composite on which we reported recently.[15] A material sush as TPD-PPV is a good candidate to study field-induced effects in the absence of the effects resulting from disorder.

Knowing that the Einstein relation is valid at low dc fields, Eqs. (25) may now be employed to calculate $\mu\tau=(5.7\pm0.5)\times10^{-9}$ cm^2/V and $L_D=114\pm5$ nm. Using $\tau=45$ μs as determined from previous photocurrent measurements we obtain a hole mobility of $\mu_{0,h}=1.3\times10^{-4}$ cm^2/V s. This value is somewhat higher than the number reported by Kulikovsky *et al.* (0.17×10^{-4} cm^2/V s, based on the analysis of photocurrent transients).[29] Since the dielectric relaxation time is also known we can use the definitions of τ_{di} and σ to estimate the quantum yield for zero external electric field Φ_0. Assuming $\varepsilon_r\approx3.5$ we obtain a value of $\Phi_0=5.6\times10^{-5}$.

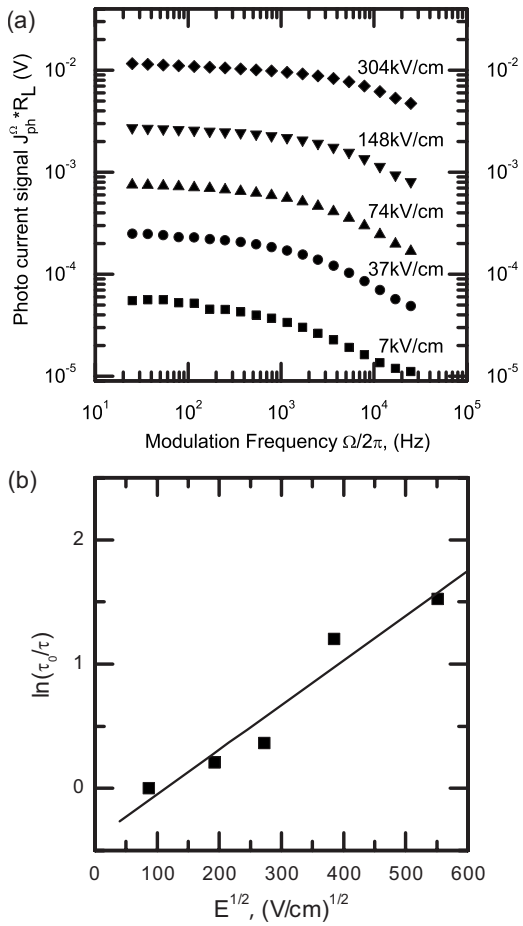

FIG. 6. (a) The frequency dependent decay of the alternating photocurrent amplitude is analyzed for different electric fields to determine the field dependence of the charge carrier lifetime. Incident intensity $I=0.4$ W/cm^2. (b) The Arrhenius plot of $\ln(\tau_0/\tau)$ versus $E^{1/2}$ is used to determine the field dependent reduction of the activation energy β.

C. High dc field

In the following we discuss the behavior of the photo-EMF signal in the high-field regime. As shown in Figs. 4 and 5 $j^{\Omega}_{p-\mathrm{emf}}$ constantly increases with increasing field after the signal has passed the minimum. The conventional model which neglects the field dependence of mobility and charge generation efficiency, however, predicts a saturation of the signal at a field of $E_0=1/(K\mu\tau)$. This is illustrated by the dashed line in Fig. 7 which represents a numerical simulation of versus field based on the conventional model (using the photophysical parameters obtained in the preceding section).

Equation (27) shows that the most important field contribution to the photo-EMF signal in our model is from the photoconductivity $\sigma(E_0)$ which is expected to increase proportional to the charge carrier generation efficiency $\Phi(E_0)$. This expectation is based on the assumption that the recombination processes in our sample are of the Langevin type which means that the $\mu\tau$ product is essentially field independent ($\tau \propto 1/\mu$ is the characteristic feature of this mechanism). The field dependence of $\Phi(E_0)$ can be determined from the ac photocurrent data shown in Fig. 4. The photocurrent amplitude was normalized to the applied electric field and fitted to Eq. (28). The resulting parameters are $a=7.4\times10^{-8}$ for the prefactor and $\alpha=1.6$ for the exponent of the power law.

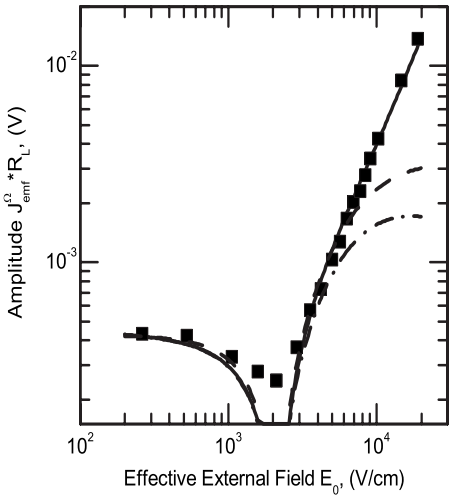

FIG. 7. Comparison of the conventional photo-EMF model (dashed line), the model assuming $\alpha=1.6$ (dotted-dashed line), and the model assuming $\alpha=2.2$ (solid line) with the experimentally obtained field dependence of the photo-EMF signal.

The lifetime-mobility relation of the Langevin mechanism can also be used to determine the field dependence of the mobility. First, the field dependence of the charge carrier lifetime was determined from photocurrent measurements versus modulation frequency at different fields [see Fig. 6(a)]. The inverse of $\tau(E_0)$ is expected to be proportional to the mobility. Indeed the change of $1/\tau(E_0)$ with field agrees with Eq. (29), i.e., $\ln 1/\tau(E_0) \propto \ln \mu(E_0)$ varies as the square root of the applied dc field [see Fig. 6(b)]. The slope of the linear fit in Fig. 6(b) is equal to $\beta=(3.5\pm0.5)\times10^{-3}$ (cm/V)$^{1/2}$.

In principle the values for α and β obtained from the photoconductivity measurements can be used with Eqs. (27) and (30) and to simulate the field dependence of the photo-EMF signal (see the dashed-dotted line in Fig. 7). However, we found that $j^{\Omega}_{p\text{-emf}}$ shows a more pronounced field dependence than expected from the above estimation. This points towards a more efficient charge generation in the photo-EMF experiment, possibly due to steady-state effects not accounted for by the ac photocurrent measurement. Leaving all other parameters unchanged and assuming $\alpha=2.2$ instead of 1.6 we found an excellent agreement of the photo-EMF signal measured at high fields with the prediction of our model (see the solid line in Fig. 7). This implies that the unusual behavior of the photo-EMF signal in the high dc field regime can be explained by a strong field dependence of the charge carrier generation efficiency. Note that the deviation between simulation and experimental data in the low-field region (1–3 kV/cm) results from the incomplete separation of the dielectric relaxation time and charge carrier lifetime, which contradicts the assumption of entirely separated characteristic times used for the derivation of Eqs. (27) and (31).

V. CONCLUSIONS

In conclusion, the non-steady-state photo-EMF effect in polymer-based organic photoconductors was extensively

studied, both theoretically and experimentally. It was demonstrated that combined with photocurrent measurements the photo-EMF technique can be successfully applied to determine the main photophysical parameters of organic photoconductors. This was achieved by developing a quantitative model for the photo-EMF effect which takes into account the specific features of these materials, in particular the strong field dependence of the mobility and charge generation efficiency. It was shown that at high dc fields the conventional model fails to describe the behavior of the photo-EMF signal as the latter is dramatically affected by the field dependence of the charge carrier generation rate. Experimental data obtained for a TPD-PPV based photorefractive material showed excellent agreement with the predictions of the theoretical model both in the low and the high dc field regime. The extracted material parameters are in good agreement with values reported in the literature. Interestingly, the Einstein law, relating carrier mobility to the diffusion coefficient, is valid for the TPD-PPV based composite studied in this work. At high dc fields the monotonic growth of the photo-EMF signal which is predicted theoretically was experimentally observed. We point out that from a practical point of view this strong field dependence of the photo-EMF signal in organic semiconductors can be useful when designing adaptive detectors for phase modulated optical signals. In fact, it was shown that the signal-to-noise ratio of non-steady-state adaptive photodetector devices is limited by the noise of output amplifier.[30] Therefore, to improve the performance of the device it is necessary to increase the absolute value of the photo-EMF signal. Although the application of a dc field has already been proposed to address this problem,[26] this method was not very successful in inorganic materials, because of the saturation of the photo-EMF signal for large values of KL_0. However, our theoretical and experimental data show that organic semiconductors are not affected by this limitation.

ACKNOWLEDGMENTS

The authors thank S. Köber and M. Salvador for experimental support and fruitful discussions. The authors would like to acknowledge H.-H. Hörhold (University of Jena) for supplying the TPD-PPV polymer and J.C. Hummelen (University of Groningen, NL) for supplying PCBM. Financial support was granted by the European Space Agency (AO99-121). One of the authors (S.M.) acknowledges additional financial support from the Humboldt Foundation.

[1] H. Hoppe and N. S. Sariciftci, J. Mater. Res. **19**, 1924 (2004).
[2] H. Sirringhaus, Adv. Mater. (Weinheim, Ger.) **17**, 2411 (2005).
[3] C. D. Muller, A. Falcou, N. Reckefuss, M. Rojahn, V. Wiederhirn, P. Rudati, H. Frohne, O. Nuyken, H. Becker, and K. Meerholz, Nature (London) **421**, 829 (2003).
[4] E. Mecher, F. Gallego-Gomez, H. Tillmann, H. H. Horhold, J. C. Hummelen, and K. Meerholz, Nature (London) **418**, 959 (2002).
[5] M. Reufer, J. Feldmann, P. Rudati, A. Ruhl, D. Muller, K. Meerholz, C. Karnutsch, M. Gerken, and U. Lemmer, Appl. Phys. Lett. **86**, 221102 (2005).
[6] J. A. Schmidt and C. Longeaud, Phys. Rev. B **71**, 125208 (2005).
[7] L. Subacius, I. Kasalynas, R. Aleksiejunas, and K. Jarasiunas, Appl. Phys. Lett. **83**, 1557 (2003).
[8] J. A. Schmidt, M. Hundhausen, and L. Ley, Phys. Rev. B **64**, 104201 (2001).
[9] M. P. Petrov, I. A. Sokolov, S. I. Stepanov, and G. S. Trofimov, J. Appl. Phys. **68**, 2216 (1990).
[10] N. Korneev, S. Mansurova, P. Rodriguez, and S. Stepanov, J. Opt. Soc. Am. B **14**, 396 (1997).
[11] H. Veenhuis, K. Buse, E. Kratzig, N. Korneev, and D. Mayorga, J. Appl. Phys. **86**, 2389 (1999).
[12] L. Mosquera and J. Frejlich, J. Opt. A, Pure Appl. Opt. **6**, 1001 (2004).
[13] C. C. Wang, R. A. Linke, D. D. Nolte, M. R. Melloch, and S. Trivedi, Appl. Phys. Lett. **70**, 2034 (1997).
[14] R. Bittner, K. Meerholz, and S. Stepanov, Appl. Phys. Lett. **74**, 3723 (1999).
[15] S. Mansurova, S. Stepanov, V. Camacho-Pernas, R. Ramos-Garcia, F. Gallego-Gomez, E. Mecher, and K. Meerholz, Phys. Rev. B **69**, 193203 (2004).
[16] H. Bässler, Phys. Status Solidi B **175**, 15 (1993).
[17] H.-H. Hörhold, H. Tillmann, D. Raabe, M. Helbig, W. Elflein, A. Bräuer, W. Holzer, and PA. Penzkofer, Proc. SPIE **4105**, 431 (2001).
[18] W. Holzer, A. Penzkofer, H. Tillmann, D. Raabe, and H. H. Horhold, Opt. Mater. **19**, 283 (2002).
[19] E. Mecher, F. Gallego-Gomez, K. Meerholz, H. Tillmann, H. H. Horhold, and J. C. Hummelen, ChemPhysChem **5**, 277 (2004).
[20] J. S. Schildkraut and Y. P. Cui, J. Appl. Phys. **72**, 5055 (1992).
[21] S. Stepanov, in *Handbook of Advanced Electronic and Photonic Materials and Devices*, edited by H. S. Nalwa (Academic, London, 2001), Vol. 2, pp. 205–272.
[22] H. E. Tseng, T. H. Jen, K. Y. Peng, and S. A. Chen, Appl. Phys. Lett. **84**, 1456 (2004).
[23] A. Hirao, H. Nishizawa, and M. Sugiuchi, Phys. Rev. Lett. **75**, 1787 (1995).
[24] R. Richert, L. Pautmeier, and H. Bässler, Phys. Rev. Lett. **63**, 547 (1989).
[25] M. Petrov, V. Bryksin, A. Emgrunt, M. Imlau, and E. Kratzig, J. Opt. Soc. Am. B **22**, 1529 (2005).
[26] S. Mansurova, S. Stepanov, N. Korneev, and C. Dibon, Opt. Commun. **152**, 207 (1998).
[27] M. Redecker, D. D. C. Bradley, M. Inbasekaran, and E. P. Woo, Appl. Phys. Lett. **73**, 1565 (1998).
[28] D. Hertel, H. Bassler, U. Scherf, and H. H. Horhold, J. Chem. Phys. **110**, 9214 (1999).
[29] L. Kulikovsky, D. Neher, E. Mecher, K. Meerholz, H. H. Horhold, and O. Ostroverkhova, Phys. Rev. B **69**, 125216 (2004).
[30] S. I. Stepanov, Appl. Opt. **33**, 915 (1994).
[31] This result also confirms that the model of a monopolar photoconductor is appropriate. In a bipolar photoconductor the amplitude of the photo-EMF signal would be reduced by a factor $\chi = (\sigma_h - \sigma_e)/(\sigma_h + \sigma_e)$ compared to the photocurrent amplitude (σ_h and σ_e are the photoconductivities of holes and electrons, respectively). This reduction is due to the competition between an electron and a hole grating with opposite signs.